

Forbidden Transitions in the Visible Spectra of an Electron Beam Ion Trap (EBIT)

E. Träbert,* P. Beiersdorfer, S. B. Utter and J. R. Crespo López-Urrutia

Department of Physics and Space Technology, Lawrence Livermore National Laboratory, Livermore, CA 94501, U.S.A.

Received March 10, 1998; accepted April 24, 1998

PACS Ref: 32.30.Jc, 34.50.Fa, 32.70.Cs

Abstract

In an explorative study of visible spectra from an electron beam ion trap (EBIT), a variety of rare-gas ion species has been excited and stored. The spectra reveal several forbidden lines and also show peculiarities of general interest to EBIT users. The lifetime of the $3s^23p^2\ ^3P_2$ level in Si-like Kr²²⁺ has been measured as $[(6.3 \pm 0.3)\text{ms}]$. The M1 transition $3s^23p^2\ ^3P_1\text{--}^3P_2$ in the Si-like ion Mo²⁸⁺ has been observed at $(284.0 \pm 0.2)\text{nm}$, confirming an identification from tokamak observations by Denne *et al.* The $3d^4\ ^5D_2\text{--}^5D_3$ transition in Ti-like Au has been found at $(353.2 \pm 0.2)\text{nm}$ and thus the predicted isoelectronic trend been confirmed.

1. Introduction

Slow radiative decays of few-electron atomic systems with level lifetimes in the range of ms to s are of interest both in fundamental atomic structure studies and in astrophysical observations. The observation and study of such decays in the laboratory requires advanced trapping techniques in order to see the radiative transitions which compete with collisional quenching. We have undertaken an explorative study of visible spectra emitted from the Lawrence Livermore National Laboratory electron beam ion trap (LLNL EBIT), aiming at spectral lines of interest for high-resolution spectroscopy at fusion test devices and astrophysical applications.

Line intensities of spin or electric-dipole forbidden transitions provide important tools in the study of elemental abundances, electron densities, and temperatures in low-density terrestrial or astrophysical plasmas by atomic spectroscopy [1, 2]. Increasingly precise calculations are available for slow forbidden decays in few-electron atomic systems [3]. In spite of the important role in plasma diagnostics of, for example, the magnetic dipole (M1) or electric quadrupole (E2) transitions between fine-structure levels in the lower configurations of many ions, there are hardly any measurements [4–6] of such forbidden transition probabilities in multicharged ions.

Forbidden lines in the visible spectrum usually have transition probabilities which relate to atomic level lifetimes in the ms range. Such ms lifetimes are (by several orders of magnitude) too long for experiments using the techniques of traditional time-resolved spectroscopy of fast ion beams [7, 8], unless they are combined with a heavy-ion storage ring [9]. In EBIT [10], ions in any charge state can be produced [11] and observed with only insignificant Doppler shift, with a detection efficiency sufficient for precision spectroscopy, and under vacuum conditions much better than in

traditional radiofrequency or electrostatic ion traps. EBITs furthermore are suitable for lifetime measurements over a very wide time range, from sub-ps and μs lifetimes [12, 13] to those of many ms [5, 14] and possibly to several seconds.

At the NIST EBIT, the spectrum of Kr in the range 320 to 460 nm has been studied [15]. The transition rate of a forbidden transition in Si-like Kr XXIII was measured [6], and another, forbidden, transition in Kr XXII was identified [15, 16]. The $3s^23p^2\ ^3P_1\text{--}^3P_2$ transition in the Si-like ion is the only such transition from an unbranched decay in $3s^k3p^l$ ions that remains in the visible or near UV for a wide range of elements, and it, therefore, is of immediate plasma spectroscopic interest [17, 18]. Besides extensions in wavelength range of the NIST work on Kr and of some earlier LLNL work on several rare gases [19], we aimed at an observation of this forbidden transition in Mo XXIX (Mo²⁸⁺) also in EBIT. We also note the observation of M1 lines in the visible at the Oxford EBIT [20].

Another transition of interest to plasma diagnostics of hot plasmas is a forbidden (M1) transition in Ti-like ions. The $3d^4\ ^5D_2\text{--}^5D_3$ transition has been predicted to show a peculiar behaviour in that over a wide range of nuclear charges it varies very little in wavelength and remains in the visible or near ultraviolet spectral range [21]. The line was duly found in EBIT spectra of several elements ($Z = 54$ to 64) [19, 20, 22, 23], and its transition probability was measured for Xe³²⁺ [5]. After semi-empirically scaled calculations [21] predicted the transition wavelength correctly within 5% for the cases covered so far, a recent *ab initio* calculation came within 1.5% of the experimental wavelengths [24]. Unfortunately, this latter calculation makes no predictions for elements not yet covered by experiment. We included in our study a search for this transition in higher- Z elements.

2. Experimental procedure

Our experiment used the SuperEBIT at Lawrence Livermore National Laboratory (LLNL). This EBIT cannot only reach electron energies up to 250 keV, which is sufficient to completely ionize uranium, but can also run at very low electron energies (below 100 eV) in the trap region, by independent adjustment of the drift tube voltage. This is a very useful feature for the steady-state production of ions not in the highest charge states. For the present work, electron energies between 80 eV and 120 keV were used, with currents up to 120 mA at the higher energies. Atoms or ions are injected into EBIT through a gas injector or a metal vapour vacuum arc ion source (MEVVA). They are stepwise ionized by electron impact in the intense electron beam which is guided and compressed to about 60 μm diameter by a

* E-mail: Traebert@ep3.ruhr-uni-bochum.de

Permanent address: Experimentalphysik III, Ruhr-Universität Bochum, D-44780 Bochum, Germany.

strong (3 T) magnetic field. The ions are then trapped, being attracted by the space charge of the electron beam, confined radially by the magnetic field and axially by suitable electric potential steps. Under appropriate vacuum conditions, the charge state reached on any element is simply determined by the ionization potential of that ion species. In the present experiment, however, the vacuum was worse (though still in the UHV range) than usual due to a developing leak in the water cooling line of the upper transport magnets. Pressures in the range up to 10^{-10} mbar led to charge state distributions that were notably affected by recombination processes, that is, they needed higher currents to reach the maximum charge states, and the charge state distributions were somewhat wider.

The trap depth was mostly 200 V for lifetime measurements, with some data runs at 100 V. The ambient pressure was $1.8 \cdot 10^{-10}$ mbar in the lower and $8 \cdot 10^{-8}$ mbar in the upper chamber of EBIT. The gas injection pressure varied from 5 to $10 \cdot 10^{-7}$ mbar. For survey spectra and wavelength measurements, the EBIT was run in a continuous mode. While the gas injector supplying material to the trap was continually open, ions were produced and accumulated for a few seconds before extraction. This extraction is necessary to prevent the build-up of unwanted residual (mostly heavy element) ion species in the trap. For the lifetime measurement, the magnetic trapping mode [14] was employed, that is alternating ionization/excitation (electron beam on) and detection (electron beam off) phases, with a 16 Hz cycle.

The light emitted from EBIT was studied by means of a 1 m normal-incidence spectrometer equipped with a 6001/mm Al/MgF₂ grating blazed for 300 nm. A 3001/mm grating was also available. The entrance slit head was removed so that the tightly confined EBIT light source could be placed at the nominal location of the entrance slit. A multichannel detector was positioned in the output focal plane, instead of the normal slit assembly. This detector was based on a 25 mm × 25 mm CCD (charge-coupled device) camera and permitted the acquisition of 40 nm wide spectra with 1024 channel resolution. Cryogenic cooling ensured a low dark rate of the detector, and the back-illuminated light-sensitive material permitted observations in a wide spectral range from vacuum-UV wavelengths to the red part of the spectrum where stray light (thermal radiation) from EBIT's electron gun limited the working range.

The spectrometer is stigmatic enough to image the length of the light source (cut to about 15 mm by the size of a window port) on the detector. This feature permitted to discriminate light emission from neutral atoms (localized in the collision zone of the gas plume from the injector with the electron beam) from that of multicarged ions (which fill the trap length) [19]. The recording of overlapping spectra provided easy means to calibrate both the mechanical spectrometer drive and the dispersion (about 0.040 nm/channel when using the 6001/mm grating) from a few prominent lines. Wavelength selection proceeded by manual setting of the spectrometer drive, and establishing the mechanical offset of the read-out from the most prominent lines in the spectra.

Working without a shutter, the CCD permitted exposure times from several seconds (data accumulation continues during the several-second read-out) to hours. Typically, every 5 to 20 min the CCD spectra were stored and a fresh

integration interval started. Random cosmic ray events usually affect a few pixels at a time and create signals on the CCD that are several orders of magnitude greater than the observed UV or optical events. A numerical filter routine was used to remove most of the associated spikes from the two-dimensional spectra. The available CCD camera, however, was not suitable for time-resolved measurement as needed to record decay times in the ms range, because the exposure could not be synchronized with modulations of the EBIT electron beam current, and because it required on the order of 10 s of read-out time after each exposure. Another problem of the CCD is a certain level of read-out noise added to the data for technical reasons. This (intentionally constant) read-out noise and the true spectral background depend differently on integration time and cannot always be disentangled.

As this type of CCD was not suitable for fast read-out or framing mode, a single channel detector (photomultiplier) was used for the intended lifetime measurements in the ms range. The low-dark rate (5 counts per second) photomultiplier tube (1/2" diameter, end-on cathode, Hamamatsu type R2557 with a 401K spectral sensitivity curve) permitted detection with more than 1% quantum efficiency from 280 to about 600 nm, or from 300 to 580 nm with more than 2.5% quantum efficiency. However, the combination of this device with the slitless normal-incidence spectrometer failed to show any strong, useful signal. This was probably due to the geometry of the normal-incidence spectrometer, which has entrance and exit slit side by side and thus the detector too close to the strong EBIT magnets, the μ -metal shielding of the detector being insufficient under the circumstances. In order to apply good light collection and reach sufficient distance, a Steinheil (glass) prism spectrograph was then employed instead and fitted with a large (10 cm diameter, f/4) collection lens (achromat), resulting in a total collection solid angle of 0.003 sr.

The CCD camera was used to find the proper optical alignment of this light collection and imaging system. Then the CCD camera was replaced by the photomultiplier. Time sorting of the detected photons with respect to the EBIT cycle was achieved by a strobe technique: The PM signal was sent to a single channel analyzer, the output of which was used in combination with a sawtooth waveform generator. An ADC in strobe mode converted the actual voltage of the sawtooth signal into an address for a data acquisition system. This ramping permitted data collection over 50 ms intervals, with a linearity of better than 0.1%.

3. Data and discussion

3.1. Spectra

Observations with Ne, Ar, Kr and CO₂ (to see carbon and oxygen lines) were tried in the range 200 to 690 nm (the range of the spectrometer – diffraction grating combination). Some of this wavelength range has been studied earlier, using a prism spectrograph and employing systematic energy variation for the identification of a number of spectral lines [19]. In the following we therefore refer to that study if possible and concentrate on our specific observations. Little light was seen below 300 nm (Fig. 1), which probably was due to a diffraction grating damaged by baking and to the lower efficiency of the CCD in this range

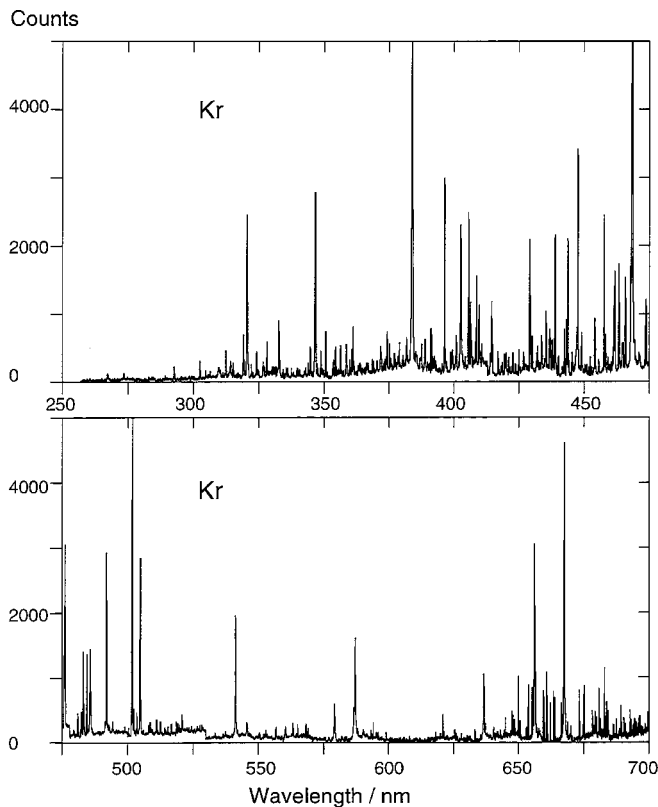


Fig. 1. Composite spectrum of Kr, recorded in 40 nm wide, overlapping sections with a CCD detector on a 1 m normal-incidence spectrometer.

rather than to the light source. However, with so little signal in the vacuum-UV, the necessity for windowless operation ceased. Thus the gas load on EBIT was reduced by separating the spectrometer from EBIT by a quartz window and restricting further studies (and most of the following discussion) to the wavelength range 280 to 690 nm. With the CCD camera the spectrometer was nevertheless evacuated. For wavelengths above 200 nm we quote the customary air wavelengths. However, at our present level of precision the difference of air or vacuum wavelengths is largely negligible.

In this visible range, the spectra showed a fair number of lines, most of the weak ones of these are unidentified. Although standard spectral tables contain very many lines from low-charge ions in this range, there was no consistent pattern of charge states or excitation levels that would permit a positive identification of even those lines that showed to be of neutral or low-charge state origin by their localized emission near the gas inlet into the trap (see above). Interspersed between those lines appeared a number of fairly intense lines which by their emission from the whole trap length were judged to originate from high-charge state ions. The standard reference tables are notably devoid of visible lines associated with highly charged ions, as such energy intervals would either correspond to transitions between high-lying levels (and these would be visible only in the absence of competing decay branches to low-lying levels) or to fine structure intervals, that is to forbidden transitions. The latter have been semiempirically systematized by Sugar and Kaufman [17, 18], but those tables cover only the $n = 2$ shell and part of the $n = 3$ shells and are incomplete at that.

Based on such predictions – which in turn lean on solar corona lines [25–27] and the like – some forbidden lines in highly charged ion have been identified in tokamak discharges (for example, see [16, 28, 29]) or other EBIT work

[15, 19, 20, 23]. A few of such lines, in particular the easily excited and very bright Kr XXIII line at 384.09 nm [16], or the Ar XIV line at 441.24 nm, were sufficient to verify the spectrometer wavelength calibration at the present level. Observation of this line at two different spectrometer settings established the dispersion and position of the CCD camera with respect to the manually set spectrometer drive and readout. The findings were then corroborated by a few further observations, and a wavelength determination to 0.4 nm was found feasible in all our spectra by straightforward reference to the spectrometer setting and the CCD channel of the line center. Closer to the reference lines, smaller uncertainties were reached.

The survey spectra of CO_2 (for the C and O spectra) showed few lines, among them the resonance lines in the Li-like ion C^{3+} ($\lambda = 154.8202/155.0774$ nm [30]) in three diffraction orders. With Ne, Ar, Kr and Cu (MEVVA with Cu and U electrodes) about 20 to 25 lines per element showed in the wavelength range 267 to 667 nm. However, many of the lines persisted from one injected gas to the next, hours or a day later. This suggests that either some materials get trapped in surfaces or recesses of the vacuum vessel and outgas for a long time, or that some of these lines do not relate at all to the gases that were leaked in. For example, Crespo *et al.* [19] found persistent contaminations with C appearing via a line cluster near 464 nm. We did not see that particular feature, but instead (among others) a line near 468.5 nm. This line would be close to (within our error bounds indistinguishable from) the $n = 3-4$ transition in some low-charge state ions, like He^+ . However, there was no notable light at the position of the $n = 2-3$ transition in the same ion. By lowering the electron energy to 90 eV, the 468.5 nm line was made to disappear, and it reappeared above 100 eV, thus indicating its production threshold. Further He^+ lines might then be the lines at 656 nm (He II 4–6) and 541 nm (He II 4–7), as well as some of the weaker lines not yet assigned. Helium contamination might be expected from the cooling system.

We also observed some of these unidentified lines to build up over time. With a freshly started EBIT they would not show, but after, say, half an hour they would appear and then persist for the rest of the run. As the spatial characteristics of their emission point to highly charged ions and thus to forbidden transitions, these mystery lines are a nuisance (possibly blending lines of interest) of possible good use: Even while their elementary association is not yet known, they might serve as auxiliary calibration lines in EBIT. For this purpose we list a few of the mystery lines in the subsequent section on Kr, as they were independent of MEVVA ion source operation.

3.1.1. Kr. Part of our spectra obtained with Kr gas leaking into EBIT is depicted in Fig. 1. Among the more prominent lines we saw lines at 309.2/310.0 nm (310 nm could be Kr XXI $^3\text{P}_0-^3\text{P}_1$, predicted at (313.4 ± 3) nm [17]), 320 nm (He II 3–5), 346.4 nm (we agree with the NIST observation of 346.47 nm [15] and concur with their identification as Kr XXII $^2\text{D}_{3/2}-^2\text{D}_{5/2}$, the weaker one of the two decay channels of the $^2\text{D}_{5/2}$ level), 384.0 nm (Kr XXIII $3s^23p^2\ ^3\text{P}_1-^3\text{P}_2$ [16]), 402.5 nm (Kr XIX [19]), 438.5 nm, 468.5 nm (He II 3–4), 491.9 nm, 501.2 nm, 540.9 nm (He II 4–7), 579.1 nm (Kr XVIII [19]), 587.1 nm, 656 nm (He II 4–6), and 667.5 nm.

The intensities of these lines by far exceeded those of the multitude of lines from low charge states (see [23, 31]) of Kr. In particular, they remained intense when lowering the gas injection pressure into EBIT, whereas the intensity of transitions from short-lived levels in low charge state ions appeared roughly proportional to pressure. Judging from the available spectroscopic tables [17, 18], the forbidden lines of wavelengths shorter than about 400 nm would most likely result from ions of charge states $q = 20+$ or higher, and they are well excited at electron beam energies of about 1.4 keV. Many of these lines appear weaker at an electron energy of 900 eV, whereas the lines above 400 nm retain their intensity. Hence we assume that many, if not most, of these lines relate to forbidden transitions in charge states lower than $q = 20$. This includes the ions with $3d^n$ electron configurations, for which little data on forbidden lines are available. Crespo *et al.* [19] have begun systematic studies of such lines using a fast prism spectrometer. We concur with their line identifications in Kr XIX (402.4 nm) and Kr XVIII (579.1 nm), but at our higher spectral resolution we see more lines which might be of interest.

3.1.2. *Si-like ions of Mo* ($Z = 42$). The $3s^2 3p^2 \ ^3P_1 - \ ^3P_2$ transition in Mo^{28+} (spectrum Mo XXIX) has previously been seen in the PLT tokamak by Denne *et al.* [29]. However, for the benefit of future studies of this line at EBIT and as a test of systematics, we tried to observe this line as well. For this purpose, the wiring of the MEVVA was changed so that instead of the main electrode material (U) ions would be produced from the Mo trigger wire. The electron beam energy was set just below the ionization potential of Mo^{28+} (1.54 keV). After about half an hour of burn-in time (to remove a possible coating of uranium on the trigger wire caused by earlier use of the MEVVA to inject uranium), a line appeared close to the predicted wavelength [17] of 283.37 nm. The line disappeared when either the electron energy dropped below the ionization potential of the next lower charge state ion, Mo^{27+} (1.45 keV), or when injection from the MEVVA was stopped, and also when the vacuum was considerably worsened (Fig. 2). All of this corroborates our charge state assignment and thus the line classification. The wavelength was determined as (284.0 ± 0.2) nm, which agrees well with the tokamak data of 284.11 ± 0.02 nm [29]. This wavelength is slightly higher than predicted, by about the same amount (0.6 nm) as was the case for the isoelectronic ion Kr^{22+} (0.8 nm) [16, 17]. Thus a straightforward correction is possible which permits

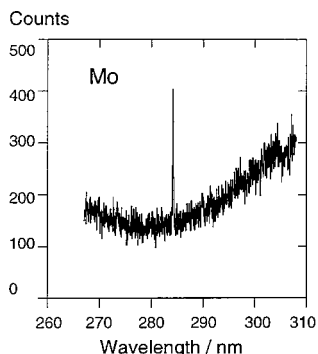


Fig. 2. Spectrum with the Mo^{28+} line of interest. The background structure is related to EBIT's thermal emission, the detector noise, and the spectrometer, but not to Mo.

a better prediction for the elements intermediate to Kr and Mo.

3.1.3. *Ti-like ions of W* ($Z = 74$), *Au* ($Z = 79$), *U* ($Z = 92$). The $3d^4 \ ^5D_2 - \ ^5D_3$ transition in Ti-like ions has been seen previously in EBIT spectra of Xe, Ba, Gd and Nd [23]. Whereas in most of the previously observed lower- Z cases the decay of the $J = 3$ level is unbranched, the $J = 2-3$ transition of interest suffers competition in very heavy ions, by the $J = 4-3$ transition which is opening up for $Z > 52$ and is taking the dominant role for $Z > 62$. The branching ratio of the wanted $J = 2-3$ transition is predicted to be only 12% in Au^{57+} and 5% in U^{70+} [21]. Although the ionization potentials of the ions of interest remain lower than 20 keV all the way up to uranium, we set the EBIT electron beam to energies from 20 to 100 keV. The metal vapour vacuum arc (MEVVA) ion source was either run with an Au cathode and a W trigger electrode, or with a U cathode and a Mo or W trigger wire. Depending on the electrical connection, either the cathode or trigger electrode material could be injected into EBIT. With Au ion injection and a 6001/mm grating, a single new line (353.2 ± 0.2) nm showed brightly in our CCD spectra which ranged from 280 to 400 nm (Fig. 3). The line appeared only when the MEVVA was firing (whereas gases like Kr may linger much longer after injection). Our data point for Au is shown with the isoelectronic trends of experiment and theory in Fig. 4.

For the corresponding search in uranium, the MEVVA was equipped with a uranium cathode in combination with a tungsten trigger electrode wire. However, although the x-ray spectra of the ions in EBIT indicated the presence of highly charged U ions, we did not detect any new line within 100 nm either side of a wavelength of 325 nm, our estimate of where the line should appear (applying an estimated offset to the prediction of 320 nm [21], based on the experimental data for lower- Z elements). This may be related to the unfavourable branching fraction of our transition of interest. Unfortunately, the wavelength of the competing $J = 4-3$ transition (predicted at 110.75 nm for U [21]) was outside our working range with the diffraction gratings available. When trying to inject W (from the trigger

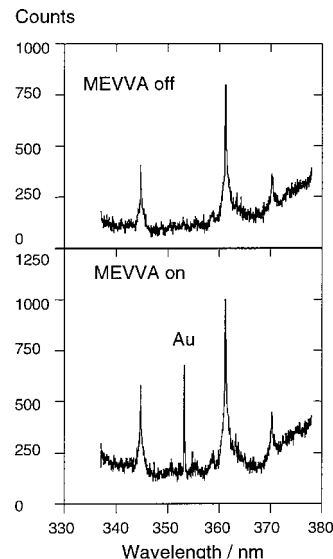


Fig. 3. Spectra near the predicted position of the forbidden $J = 2-3$ transition in Ti-like Au^{57+} . The line of interest clearly shows in the spectrum with ion injection from the MEVVA ion source (top) and is absent otherwise (bottom). The identity of the background gas lines is not known.

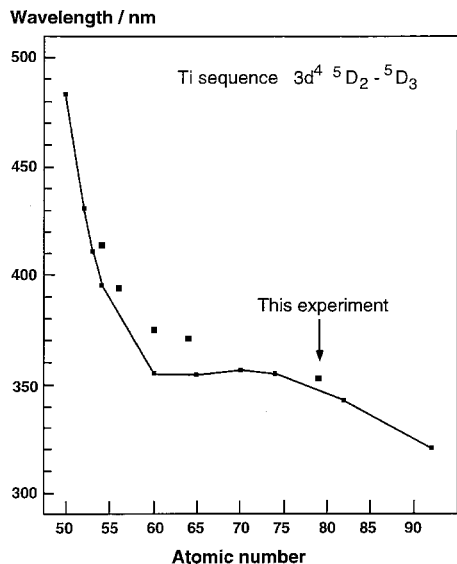


Fig. 4. Isoelectronic sequence of Ti, wavelength of the transition $3d^4 5D_2 - 5D_3$. Theory data [21] are connected by an eye-guiding line; Experiment: Data for $Z = 54$ to 64 [20, 22], datum for $Z = 79$ is from this work.

wire) into EBIT, there was only some diffuse weak spectral feature near the predicted position, too uncertain to claim positive identification.

3.2. Decay curves

Decay curves were recorded only on one line, the $3s^2 3p^2 3P_1 - 3P_2$ transition of the Si-like ion Kr^{22+} , at a wavelength of 384 nm. Data were collected over 50 ms intervals and sorted by the time of event after the electron beam was switched off so that EBIT was being run in magnetic trapping mode [5, 14]. In this mode the ions are still confined radially by the magnetic field and longitudinally by the

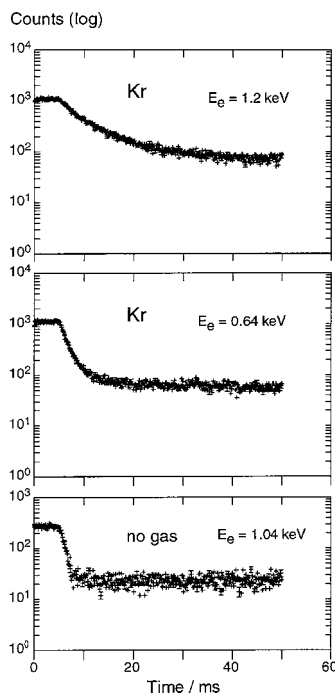


Fig. 5. Decay curves observed with Kr ions at $\lambda = 384$ nm. Isoelectronic sequence of Si, transition $Kr^{22+} 3s^2 3p^2 3P_1 - 3P_2$. The electron beam is switched off at $t = 5$ ms. Top: Electron energy 1.2 keV (above threshold for the production of Kr^{22+} ions), middle: Electron energy 640 eV (just above threshold for the production of Kr^{18+} ions). Bottom: Electron energy 1.04 keV, no gas injection.

trap electrodes; the disappearance of the attractive and space-charge compensating electron beam results in a sudden expansion step of the ion cloud. This step is as fast as the switching of the electron beam current and does not affect the decay curves at later times.

Decay curves were recorded at various electron beam energies, from 1.4 keV (well above the 1.0 keV ionization energy of Kr^{22+}) to 648 eV (just above the production threshold of Kr^{18+}). The latter measurement was done because there was light even at lower electron energies than the production threshold for Kr^{22+} . We interpret this light to arise from the 402.5 nm line of Ar-like Kr^{18+} [19], which was marginally in the field of view of the 1/2" diameter photomultiplier tube attached (without an exit slit) to the prism spectrograph. This line was not seen in the CCD spectra obtained when setting up using electron energies of 1.4 keV, but may well have come up at energies below 1 keV. Even without gas injection, a signal with a time constant of about 0.8 ms was seen, which is slower than the about 50 μ s switching time of the electron gun. A component of this time constant was corrected for in the decay curves taken with gas injection. Below the production threshold for Kr^{22+} , a dominant time constant of order 2 ms was seen which we ascribe to the branched M1 decay in Kr^{18+} [19]. At the higher excitation energies the observed signal is dominated by the wanted line in Kr^{22+} , but it will be contaminated by the other two contributions, which can only approximately be accounted for.

Total collection time for about 10 curves of a statistical quality comparable to those shown in Fig. 5 was about 24 h. The total number of counts in the decay part of the data, after background subtraction, was of order 30 000, permitting in principle the determination of lifetimes with statistical uncertainties below 1%. Decay constants were determined for the individual runs, which extended over about 5 $1/e$ lifetimes, by least-squares fits of one or two exponentials plus a constant background to each of the observed decay curves. For all data samples, the start of the fit range was varied between 0.5 and 10 ms after switching off the electron beam. The error estimates were derived from the least-squares fit, augmented by estimates of error due to the spectral blend. The fitted decay constants from the individual runs fluctuate as expected for their statistical errors, the weighted averages yielding a mean value for the lifetime of (6.3 ± 0.3) ms or a transition probability of (160 ± 8) s^{-1} for the $3s^2 3p^2 3P_2$ level of Kr^{22+} .

The lifetime result agrees with that obtained at NIST $\{(5.7 \pm 0.5)$ ms [6]. However, due to better signal yield, our data have reached a smaller uncertainty of only 5%. The two theoretical lifetime numbers available, 6.46 ms [32] and 5.83 ms [33], both require semiempirical adjustment for the transition energy, because the M1 transition probability depends on ΔE^3 (see also Ref. [34]). After such a correction, they are at 6.78 ms and 6.69 ms, respectively (see discussion in [6]), which is outside our error estimate. A semi-empirical analysis of such (dominantly) M1 transitions in Si-like ions, that links spectroscopic level structure and transition rates, has been presented by Curtis [35]. With such good light collection as used here, but better spectral filtering, we expect to be able to improve the experiment in the future. A long term goal would be a measurement precise enough to probe the E2 contribution to the transition amplitude.

4. Outlook

The SuperEBIT at LLNL is equipped with an electron gun that can deliver electrons at energies up to 250 keV, so that any charge state of any element can be reached. Present plasma devices for fusion research, however, do not need data in that full range, nor are the visible envelopes and coronae of stars so hot as to feature extremely high ionization stages. Therefore data for practical analyses of terrestrial and stellar plasmas are needed of multi-, but not necessarily very highly, charged ions. SuperEBIT is particularly well suited for this task, as it is uniquely flexible also in reaching very low electron energies (below 100 eV) in the trap region.

The combination of a normal-incidence spectrometer equipped with a CCD camera proved very simple to use and at the same time very efficient for survey spectra of ions produced and stored in an electron beam ion trap. It takes advantage of the resolution obtainable with grating spectrometers as well as of the sensitivity and multichannel, wide spectral range, low-noise capabilities of the CCD. The present technique can easily be extended to systematic surveys of forbidden transitions in many ion spectra, in particular to those of interest in astrophysics and plasma diagnostic. For the probabilities of forbidden transitions, this study covered a particularly bright specimen and improved on the available data. For the more usual less bright lines, a very efficient light collection and detection system is required. However, with such a system, lifetime measurements in the ms range with uncertainties in the few-percent range seem quite feasible for a variety of highly charged ions.

Acknowledgement

J. Steiger deserves thanks for the loan of the photomultiplier. E.T. appreciates the travel support granted by the Humboldt Foundation and the support and the hospitality extended by the LLNL EBIT group. The work at Lawrence Livermore National Laboratory was performed under the auspices of the Department of Energy under Contract No. W-7405-Eng-48.

References

1. Doschek, G. A., in: "Autoionization" (Edited by A. Temkin) (Plenum, New York 1985), p. 171.
2. Edlén, B., *Physica Scripta* **T8**, 5 (1984).
3. Lindroth, E., *Nucl. Instrum. Meth.* **B98**, 1 (1995).
4. Yang, L., Church, D. A., Tu, S. and Jin, J., *Phys. Rev.* **A50**, 177 (1994).
5. Serpa, F. G. *et al.*, *Phys. Rev.* **A55**, 4196 (1997).
6. Serpa, F. G., Gillaspay, J. D. and Träbert, E., *J. Phys.* **B31**, 3345 (1998).
7. Träbert, E., *Physica Scripta* **48**, 699 (1993).
8. Träbert, E., in: "Accelerator-based Atomic Physics Techniques and Applications" (Edited by S. M. Shafroth and J. C. Austin) (*Am. Inst. Phys.*, Washington 1997), p. 567.
9. Doerfert, J., Träbert, E., Wolf, A., Schwalm, D. and Uwira, O., *Phys. Rev. Lett.* **78**, 4355 (1997).
10. Marrs, R., Beiersdorfer, P., Elliott, S. R., Knapp, D. A. and Stöhlker, Th., *Physica Scripta* **T59**, 183 (1995).
11. Marrs, R., Elliott, S. R. and Knapp, D. A., *Phys. Rev. Lett.* **72**, 4082 (1994).
12. Beiersdorfer, P., Ostenheld, A. L., Decaux, V. and Widmann, K., *Phys. Rev. Lett.* **77**, 5353 (1996).
13. Wargelin, B. J., Beiersdorfer, P. and Kahn, S. M., *Phys. Rev. Lett.* **71**, 2196 (1993).
14. Beiersdorfer, P., Schweikhard, L., Crespo López-Urrutia, J. and Widmann, K., *Rev. Sci. Instrum.* **67**, 3818 (1996).
15. Serpa, F. G., Bell, E. W., Meyers, E. S., Gillaspay, J. D. and Roberts, J. R., *Phys. Rev.* **A55**, 1832 (1997).
16. Roberts, J. R., Pittman, T. L., Sugar, J., Kaufman, V. and Rowan, W. L., *Phys. Rev.* **A35**, 2591 (1987).
17. Sugar, J. and Kaufman, V., *J. Opt. Soc. Am.* **B1**, 218 (1984).
18. Kaufman, V. and Sugar, J., *J. Phys. Chem. Ref. Data* **15**, 321 (1986).
19. Crespo López-Urrutia, J. R., Beiersdorfer, P., Widmann, K. and Decaux, V. (in preparation); Crespo López-Urrutia, J. R., Beiersdorfer, P., Widmann, K. and Decaux, V., in: "Nineteenth International Conference on the Physics of Electronic and Atomic Collisions – Scientific Program and Abstracts of Contributed Papers" (Edited by J. B. A. Mitchell, J. W. McConkey and C. E. Brion) (ICPEAC, Whistler, BC 1995), p. 589.
20. Bieber, D. J., Margolis, H. S., Oxley, P. K. and Silver, J. D., *Physica Scripta* **T73**, 64 (1997).
21. Feldman, U., Indelicato, P. and Sugar, J., *J. Opt. Soc. Am.* **B8**, 3 (1991).
22. Morgan, C. A. *et al.*, *Phys. Rev. Lett.* **74**, 1716 (1995).
23. Serpa, F. G. *et al.*, *Phys. Rev.* **A53**, 2220 (1996).
24. Beck, D. R., *Phys. Rev.* **A56**, 2428 (1997).
25. Edlén, B., *Z. Astrophysik* **22**, 30 (1942).
26. Smitt, R., *Solar Phys.* **51**, 113 (1977).
27. Jordan, C., in: "Progress in Atomic Spectroscopy B" (Edited by W. Hanle and H. Kleinpoppen) (Plenum, New York 1979), p. 1453.
28. Denne, B., Hinnov, E., Ramette, J. and Saoutic, B., *Phys. Rev.* **A40**, 1488 (1989).
29. Denne, B., Hinnov, E., Suckewer, S. and Cohen, S., *Phys. Rev.* **A28**, 206 (1983).
30. Kelly, R. L., "Atomic and Ionic Spectrum Lines below 2000 Å, H through Ar" (Oak Ridge National Laboratory, Oak Ridge 1982).
31. Das, M. B., *J. Quant. Spectrosc. Rad. Transfer* **57**, 237 (1997).
32. Biémont, E. and Bromage, G. E., *Mon. Not. R. Astron. Soc.* **205**, 1085 (1983).
33. Huang, K.-N., *At. Data Nucl. Data Tables* **32**, 503 (1985).
34. Mendoza, C. and Zeippen, C. J., *Mon. Not. R. Astron. Soc.* **199**, 1025 (1982).
35. Curtis, L. J., *Phys. Rev.* **A39**, 6958 (1989).